


## Article

# Super Porous Carboxymethyl Cellulose–Tannic Acid (TA@CMC) Cryogels with Antioxidant, Antibacterial, and $\alpha$ -Glucosidase Enzyme Inhibition Abilities

Mehtap Sahiner<sup>1,2</sup> , Sahin Demirci<sup>3,4</sup> and Nurettin Sahiner<sup>4,5,6,\*</sup>

<sup>1</sup> Department of Bioengineering, Engineering Faculty, Canakkale Onsekiz Mart University, Terzioğlu Campus, Canakkale 17100, Turkey; sahinerm78@gmail.com

<sup>2</sup> Department of Chemical and Biomedical Engineering, and Materials Science and Engineering, University of South Florida, Tampa, FL 33620, USA

<sup>3</sup> Department of Food Engineering, Faculty of Engineering, Istanbul Aydin University, Florya Halit Aydin Yerleşkesi, Istanbul 34295, Turkey; sahind@aydin.edu.tr or sahindemirci@gmail.com

<sup>4</sup> Department of Chemistry, Faculty of Sciences, Canakkale Onsekiz Mart University, Terzioğlu Campus, Canakkale 17100, Turkey

<sup>5</sup> Department of Ophthalmology, Morsani College of Medicine, University of South Florida, 12901 Bruce B. Downs Blvd, MDC21, Tampa, FL 33612, USA

<sup>6</sup> Department of Bioengineering, U.A. Whittaker College of Engineering, Florida Gulf Coast University, Fort Myers, FL 33965, USA

\* Correspondence: nsahiner@fgcu.edu or sahinerm71@gmail.com

**Abstract:** Here, super porous carboxymethyl cellulose (CMC) cryogels were synthesized in 10–100% crosslinker and the presence of TA, at varying amounts of TA, e.g., 10 and 25 wt% of CMC under cryogenic conditions ( $-20\text{ }^{\circ}\text{C}$ ) as TA@CMCs. To control the degradation of CMC cryogel networks, the crosslinking ratio of divinyl sulfone (DVS:X) to CMC varied at 10, 25, 50, and 100% moles of the CMC repeating unit. Higher hydrolytic degradation was observed for CMC 10%X cryogels at pH 1.0 with  $28.4 \pm 1.2\%$  weight loss. On the other hand, the TA-release studies from TA@CMC-based cryogels showed that higher TA releases were observed for both TA@CMC 10% and 25% cryogels at pH 7.4, with  $23.6 \pm 1.1$ , and  $46.5 \pm 2.3\text{ mg/g}$  in 480 min, which are equal to almost 24% and 18% of the TA contents of the corresponding cryogels, respectively. The antioxidant properties of TA@CMC cryogels were examined, and worthy antioxidant properties were observed due to the TA. The alpha-glucosidase enzyme inhibition ability of the prepared cryogels was examined at different concentrations by grinding cryogels, and it was determined that TA@CMC 25% cryogel at 3 mg/mL concentration inhibited  $70.4 \pm 1.3\%$  of the enzyme. All bare CMC-based cryogels were found to be non-hemolytic with a less than 1% hemolysis ratio and also effective on the blood coagulation mechanism with blood-clotting index (BCI) values between 62.1 and 81.7% at 1 mg/mL concentrations. On the other hand, TA@CMC 25% cryogels exhibited a slight hemolytic profile with a  $6.1 \pm 0.8\%$  hemolysis ratio and did not affect the blood coagulation mechanism with  $97.8 \pm 0.4\%$  BCI value.

**Keywords:** carboxymethyl cellulose; tannic acid; cryogel; biodegradable; polysaccharide cryogels



**Citation:** Sahiner, M.; Demirci, S.; Sahiner, N. Super Porous Carboxymethyl Cellulose–Tannic Acid (TA@CMC) Cryogels with Antioxidant, Antibacterial, and  $\alpha$ -Glucosidase Enzyme Inhibition Abilities. *Polysaccharides* **2024**, *5*, 823–841. <https://doi.org/10.3390/polysaccharides5040051>

Academic Editors: Jungmok You and Cédric Delattre

Received: 9 May 2024

Revised: 29 August 2024

Accepted: 3 December 2024

Published: 6 December 2024



**Copyright:** © 2024 by the authors. Licensee MDPI, Basel, Switzerland. This article is an open access article distributed under the terms and conditions of the Creative Commons Attribution (CC BY) license (<https://creativecommons.org/licenses/by/4.0/>).

## 1. Introduction

The technique of cryogelation has gained tremendous recognition in the last decade, and numerous researchers have focused on the application of polymer cryogel in various disciplines including biotechnology and biomedicine [1–5]. For example, poly(2-hydroxyethyl methacrylate) cryogel is used for protein immobilization and cell separation [6,7], while DNA cryogel is used to remove carcinogens [6,7]. Polyvinyl alcohol cryogel is employed in orthopedic devices, intervertebral discs, cardiovascular devices, cartilage, and even medical imaging [8–11]. Fibrin cryogel is used as a scaffold [10–12]. Biodegradable materials were used to prepare cryogels, resulting in successful applications

in bone-tissue engineering, hemostasis and wound healing, enzyme immobilization, drug carriers, delivery vehicles, and bioactive component applications [12–14].

Among cellulose derivatives, carboxymethyl cellulose (CMC) is one of the most promising polysaccharides with attractive physical and chemical properties. It is widely used in numerous applications such as food, paper, textile, and pharmaceutical industries, biomedical engineering, wastewater treatment, energy production and storage, and so on. The low-cost synthesis process and adjustable hydrophilicity, viscous properties, mechanical strength, availability and abundance of raw materials, and unique surface properties are some of the appealing aspects [15–17]. Therefore, CMC-derived materials in different formulations and sizes possess tunable performance, including solubility, particle size, viscosity, and rheological properties, which are related to the purity, degree of polymerization (DP), degree of substitution (DS), uniformity, and so on playing an important impact on the application of CMC in different areas [15,18,19]. Carboxymethyl cellulose (CMC) is used as a thickener in foods such as dairy products and bakery products. Also, in eye drops, CMC has functions such as a humidifier and lubricant for dry eyes. CMC microspheres were synthesized with glutardialdehyde for environmental application, e.g., dye adsorption [20]. In another study, CMC was crosslinked with citric acid as a wound-healing hydrogel [21].

Tannic acid (TA) constructed from ten gallic acid molecules joining to a central glucose unit is a naturally occurring tannin that belongs to the group of phenolic acids [22]. One of the primary examples of a tannin that can be effectively extracted from natural sources with high efficiency is tannic acid (TA), which is of great interest to scientists. TA has been investigated as a naturally active material in polymeric particle preparation, or as a biopolymer crosslinker [23,24]. TA possesses multifunctional properties by targeting multiple oncogenic signaling pathways and functioning as a cell cycle regulator in various malignancies [25]. TA has much potential as a cost-effective and safe anticancer agent for lung and breast cancer treatment [26]. Tannic acid has a lot of exclusive qualities such as being anticancer/antimutagenic [27] and able to fight against germs, including viruses and bacteria [28–30], and it can also be used as a homeostatic agent and antioxidant material [31–34]. TA is also used as an organic polymer additive due to its ability to expose bioactive characters and to improve the qualities of materials intended for use in biomedical applications [25,35–37].

In this study, an interconnected super porous cryogel network was successfully prepared, employing carboxymethyl cellulose (CMC) as a biodegradable and natural precursor via cryo-crosslinking reactions in the presence of various amounts of divinyl sulfone (DVS) as a crosslinker under cryogenic conditions ( $T = -20\text{ }^{\circ}\text{C}$ ). Moreover, the CMC-based cryogels were prepared in the presence of 10, 25, 50, and 100 mole% of tannic acid (TA) based on CMC repeating as TA@CMC. The hydrolytic degradation of CMC-based cryogels and the TA-release profiles of TA@CMC cryogels were studied at three different buffer solutions that represent the biological environments, i.e., at pH 1.0 (stomach), 7.4 (plasma), and 9.0 (intestine). The antioxidant properties of TA@CMC cryogels were determined according to the different antioxidant tests, and their  $\alpha$ -glycosidase enzyme inhibition capabilities were examined. Moreover, the antimicrobial properties of TA@CMC cryogels were tested against Gram-positive and Gram-negative bacterial strains. Furthermore, the blood compatibility of CMC-based cryogels was investigated via hemolysis and blood-clotting index assays at 1 mg/mL concentrations, and the cytotoxicity of CMC-based cryogels was tested against L929 fibroblast cell lines in the presence of 1 mg of cryogels.

## 2. Materials and Methods

### 2.1. Materials

Carboxymethyl cellulose sodium salt (CMC, high viscosity, 800–3100 mPas, Milipore) and tannic acid (TA, Sigma-Aldrich) were used for CMC cryogels. Divinyl sulfone (DVS, >96%, TCI, Tokyo, Japan) was used as a crosslinker agent.

Folin–Ciocalteu’s phenol reagent (99% purity, Sigma-Aldrich, USA), sodium nitrite (97% purity, Acros), and aluminum chloride (99.9% purity, Alfa-Aesar, USA) were used for conducting the antioxidant test. For the enzyme inhibition tests,  $\alpha$ -glucosidase from *Saccharomyces cerevisiae* (Sigma-Aldrich) and substrate p-nitrophenyl- $\alpha$ -D-glucopyranose ( $\geq 99\%$  purity, Sigma-Aldrich) were employed. The antibacterial activity tests were conducted using Gram-negative bacteria *E. coli* (ATCC 8739) and Gram-positive bacteria *S. aureus* (ATCC 6538), which were derived from KWIK-STIK™ Microbiologics (St. Cloud, MI, USA). The growth mediums for bacteria, such as nutrient agar (NA, BD Difco™ (Becton, Dickinson and Company, Sparks, MD, USA)) and nutrient broth (NB, RPI, Research Products International, Mt Prospect, IL, USA) were procured.

## 2.2. Synthesis of CMC and TA@CMC Cryogels

To synthesize CMC cryogels, the previously reported method by our group was followed with slight modification [38,39] and given in Figure 1. In brief, a certain amount of CMC, 0.4 g, was dissolved in 12 mL of 0.2 M NaOH for approximately two hours to prepare the CMC cryogel. The solutions were then cooled for three minutes in a deep freezer at  $-20\text{ }^{\circ}\text{C}$ . Different volumes of DVS, equivalent to 10, 25, 50, and 100% moles of repeated unit of CMC were added to the CMC precursors, respectively. The mixture was then vortexed and rapidly poured into cylindrical plastic syringes with a 1.5 cm diameter. After that, the mixture was frozen for 24 h at  $-20\text{ }^{\circ}\text{C}$  to initiate the cryo-crosslinking process. Following the cryogel preparation, the material was taken out of the syringe, diced into a cylindrical shape with a length of 0.5 mm, and washed with DI water for 4 h, changing the wash water every hour. The prepared cryogels were dried in an oven at  $50\text{ }^{\circ}\text{C}$  following the washing process. The prepared CMC-based cryogels crosslinked 10, 25, 50, and 100 mole% DVS were labeled as CMC 10%, CMC 25%, CMC 50%, and CMC 100% X cryogels, respectively. The crosslinking of CMC polymers with DVS was performed under basic conditions via a Michael-type addition reaction between the direct interaction of vinyl groups of DVS and hydroxyl groups of CMC chains, resulting in the formation of the CMC network under cryogenic conditions.

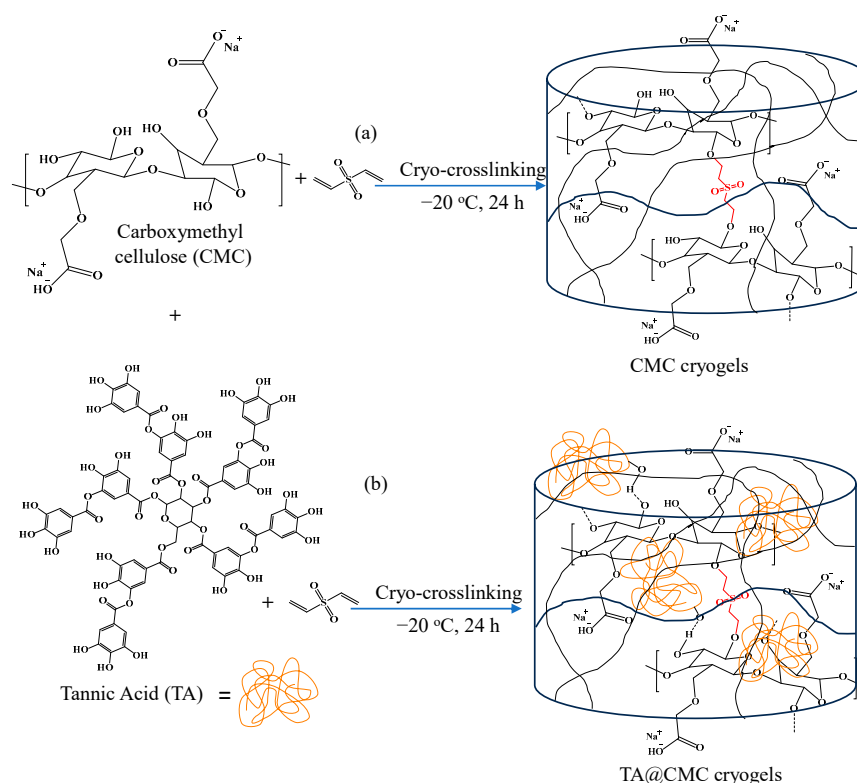


**Figure 1.** The schematic depiction of synthesis of (a) CMC-based cryogels and (b) TA@CMC cryogels.

To prepare TA@CMC cryogels, 0.4 g of CMC was weighed in a vial. Then, 0.04 and 0.1 g of TA were added to the CMC separately, representing 10% and 25% of the total weight of CMC. Next, a separate 12 mL 0.2 M NaOH solution was added to each vial, and it took roughly two hours for it to dissolve. The solutions were then cooled for three minutes in a deep freezer at  $-20\text{ }^{\circ}\text{C}$ . Afterwards, 60  $\mu\text{L}$  of DVS, 100 mol% CMC repeating unit, was added to the mixture as a crosslinker, and, after vortex mixing, the mixture was quickly poured into cylindrical plastic syringes with a diameter of 1.5 cm. The mixture was then placed to  $-20\text{ }^{\circ}\text{C}$  for about 24 h for cryo-crosslinking processes. The prepared TA@CMC cryogels were removed from the syringe, cut in a similar shape of 0.5 mm of length, and directly dried in an oven at  $50\text{ }^{\circ}\text{C}$  without the washing step to prevent TA losses. The prepared TA@CMC cryogels contain 10 and 25 wt% TA; they were labeled as TA@CMC 10% and TA@CMC 25%, respectively.

The cryo-crosslinking method that utilizes the ice crystals under freezing conditions, leading to super porous structures, was employed to prepare CMC-based cryogels. Using DVS as a crosslinker, the CMC chains were crosslinked in a three-dimensional (3D) porous network. Figure 1a illustrates the schema of the prepared CMC-based cryogels using DVS as the crosslinking agent. TA-embedded CMC cryogels (TA@CMC) with different amounts of TA were also prepared with the same procedure used in CMC cryogel synthesis. The TA molecules were included in the CMC precursors during the synthesis, and the corresponding scheme is also given in Figure 1b. The cryo-crosslinking reactions of CMC chains with DVS were carried out in the presence of TA to entrap TA molecules within the CMC network. The amount of TA was determined as 10 and 25 wt% based on the used amount of CMC during synthesis. Any further attempt to increase the amounts of TA within CMC cryogels, e.g., 50 and 100% by weight of CMC, was not successful and did not form a cryogel network. The crosslinking reaction of CMC's functional groups, e.g., -OH with DVS, was carried out by means of Michael-addition reaction in a basic medium. Therefore, CMC was dissolved in 0.2 M of NaOH to activate the relevant functional groups. However, the strength of 0.2 M of NaOH was not enough to obtain a basic medium in the presence of higher amounts of TA. Therefore, it was assumed that TA@CMC cryogels with TA amounts of  $\geq 50$  wt% of CMC could not be synthesized in 0.2 M NaOH solution.

### 2.3. Characterization of CMC and TA@CMC Cryogels

Scanning electron microscopy (FIB SEM, QUANTA 200 3D, FEI, Hillsboro, OR, USA) and an optical microscope (Olympus, BH-2, Tokyo, Japan) were used to image the TA@CMC cryogels. TA@CMC cryogels were mounted on carbon-tape-attached aluminum SEM stubs and vacuum-coated with gold to a thickness of a few nanometers, and the SEM images were captured at 30 kV. FT-IR spectroscopy (Nicolet IS10, Thermo, Waltham, MA, USA) was employed to the functional group analysis of CMC and TA@CMC-based cryogels in the  $4000\text{--}650\text{ cm}^{-1}$  wavelength range. Elemental analyses of CMC-based cryogels were carried out via an elemental analyzer (LECO, CHNS-932, Marlton, NJ, USA).

The swelling%, porosity%, pore volume ( $V_p$ ), and gel yield% of CMC-based cryogels were calculated using the following equations:

$$\text{Swelling\%} = [(m_s - m_d)/m_d] \times 100 \quad (1)$$

$$\text{Porosity\%} = [(m_s - m_d)/(m_s - m_{sq})] \times 100 \quad (2)$$

$$\text{Pore volume} = (m_{ch} - m_d)/(m_d \times d_{ch}) \quad (3)$$

$$\text{Gel yield\%} = (m_d/m_r) \times 100 \quad (4)$$

Here, " $m_s$ " is the weight of the cryogel pieces swollen in water, " $m_d$ " is the weight of the washed and freeze-dried cryogel pieces, " $m_{sq}$ " is the weight of the cryogel pieces extruded after swelling in water, " $m_{ch}$ " represents the weight of cryogel blown in cyclohexane, " $d_{ch}$ " represents the density of cyclohexane, and " $m_r$ " is the weight of the total amount of cryogel precursors.

#### 2.4. Hydrolytic Degradation of CMC-Based Cryogels

The hydrolytic degradation profiles of CMC-based cryogels were investigated in buffer solutions at pH values of 1.0 (hydrochloric acid–potassium chloride buffer), 7.4 (phosphate buffer), and 9.0 (borate buffer). Briefly, 30 mg of CMC-based cryogels was placed into 30 mL of buffer solutions at different pH values. The mixture was then kept in a water bath at 37.5 °C. The dry cryogels were weighted gravimetrically before being placed in buffer solution; after that, at fixed time intervals at 1–7 days, they were removed from the buffer solution and weighted to assess the hydrolytic degradation extent of the CMC-based cryogels according to Equation (5):

$$\text{Hydrolytic degradation\%} = [(m_{di} - m_{dt})/m_{di}] \times 100 \quad (5)$$

where “ $m_{di}$ ” is used to define the weight of dry CMC-based cryogel at the initial state, and “ $m_{dt}$ ” is used to define the weight of CMC-based cryogels kept in related buffer solution and dried in oven for 24 h. The hydrolytic degradation studies were carried out in triplicate, and the results were presented with the corresponding standard deviations.

#### 2.5. TA-Release Profiles of TA@CMC Cryogels

The TA-release profile of TA@CMC cryogels containing varying amounts of TA content, 10% and 25% CMC by weight, was investigated using three different pH buffers. The TA-release profiles from the TA@CMC cryogels were measured at 37.5 °C by gravimetrically soaking 30 TA@CMC mg for the duration of 480 min in 30 mL buffer solution at pH 1.0 (potassium chloride–hydrochloric acid buffer), pH 7.4 (phosphate buffer), and pH 9.0 (borate buffer). Using UV–Vis spectroscopy (UV–Vis Spectrophotometer, Genesys 180, ThermoScientific, USA), the maximum absorption wavelength of TA was measured at 276 nm for pH 1.0 and pH 7.4 and at 300 nm for pH 9.0; the amount of TA released was determined based on the previously prepared calibration curve for TA. After removing 0.5 mL of the release medium from each sample, the matching fresh medium was added, and the absorbance values at the specified wavelengths were noted. The TA release was carried out in triplicate, and the results were reported with the corresponding standard deviations. The related equation was given in Equation (6):

$$\text{TA release} = (C_t \times \text{DF} \times \text{volume of buffer})/\text{g of cryogel} \quad (6)$$

where  $C_t$  is the concentration of the released TA at  $t$  time, DF is the dilution factor, and the volume of buffer is in liters, respectively.

#### 2.6. Determination of Bioactive Properties of TA@CMC Cryogels

According to the literature, the total phenol content (FC) of the TA@CMC cryogels was assessed. Briefly, 2000 µg/mL of TA@CMC cryogels was prepared and mixed overnight at 500 rpm. Several dilutions of this suspension solution were performed in the range of 125–1000 µg/mL. In a 96-well plate, 20 µL of sample solution was placed, and 125 µL of FC solution was added. Subsequently, incubation was carried out in the dark for two hours with 100 µL of an aqueous 0.7 M  $\text{Na}_2\text{CO}_3$  solution. A microplate reader (Thermo Scientific, Multiskan SKY, Waltham, MA, USA) was used to read the solutions at 760 nm. The values were reported as gallic acid (GA) equivalents using GA as the calibration curve [40].

The total phenol, total flavonoid, and ferrous-reducing antioxidant assays of TA@CMC cryogels were also examined in the range of 125–2000 µg/mL according to the literature [40]. The Fe(II) chelating activity was examined in the DI water in the 31.25 and 1000 µg/mL concentration range [40]. The antimicrobial ability of TA@CMC cryogels was examined in the 10–0.625 µg/mL range against two bacterial species. At the end of 24 h incubation, the MIC value was determined, and then nutrient broth cultivation for MBC was performed.

The effect of CMC and TA@CMC cryogels on  $\alpha$ -glucosidase activity was determined, employing the method reported in the literature [40]. The TA@CMC cryogels were ground

at 3000 µg/mL concentration in 67 mM potassium buffer solution, pH 6.9. The details of the procedure are given in the supporting information.

In the biocompatibility test, 1 mg cryogel portions were dropped into 100 µL DMEM solution, and, upon 24 h incubation time, the cell viability against L929 human fibroblast cells was determined according to the literature [41]. The relevant information for the cytotoxicity of CMC and TA@CMC cryogels is also given in the supporting information.

### 2.7. Statistical Evaluation

Using GraphPad Prism 10 software, the statistical analysis of the pore sizes of CMC-based cryogels was analyzed using Dunnett's multiple-comparison test and one-way ANOVA. Bare CMC-based cryogels were used as control over TA@CMC 10% and TA@CMC 25% cryogels. A *p*-value < 0.05 was considered statistically significant.

## 3. Results and Discussion

### 3.1. Characterization of CMC-Based Cryogels

The FT-IR spectrum of linear CMC and crosslinked CMC cryogels is shown in Figure 2. The characteristic peaks for the CMC were observed at the stretching vibrations of 3500–3000 cm<sup>-1</sup>, 2912 cm<sup>-1</sup>, 1587 cm<sup>-1</sup>, and 1414 cm<sup>-1</sup>, which are attributed to the -OH, -CH, and -COOH groups, respectively, of the CMC. In the FT-IR spectrum of crosslinked CMC cryogels, there are slight variations for the peaks at 1288 cm<sup>-1</sup>, 1105 cm<sup>-1</sup>, and 1050 cm<sup>-1</sup>, which are due to the stretching vibrations of the S-O groups coming from the DVS crosslinker. In the spectrum of TA, a broad band at 3308 cm<sup>-1</sup> corresponds to the polyphenol -OH stretching.

The C=O groups are responsible for the absorption peak at 1699 cm<sup>-1</sup> in the FT-IR spectra of TA. Three more characteristic peaks are observed at 1606 cm<sup>-1</sup>, 1532 cm<sup>-1</sup>, and 1443 cm<sup>-1</sup>; these are due to the stretching of aromatic compounds, and peaks at 1180 cm<sup>-1</sup>, 1082 cm<sup>-1</sup>, and 1016 cm<sup>-1</sup> are due to the vibration of the substituted benzene rings of TA molecules. From the FT-IR spectra of the TA@CMC cryogel, as the amount of TA increased, the -OH bands became more pronounced. These observations are consistent with reports in the literature containing CMC and TA molecules. As the interactions between CMC-TA via physical hydrogen bonds are present, TA@CMC cryogels also possess the characteristic peaks coming from both CMC and TA structures [42]. On the other hand, thermogravimetric analyses (TGAs) of CMC and CMC-based cryogels were also reported in the literature to compare the thermal stability of the structures [39,43]. The significant thermal degradation of the CMC started at 240 °C, resulting in a 14.34% weight loss. This weight loss was mainly due to the inorganic components. Furthermore, a slight weight loss, 4.61%, was observed in the 154–202 °C range [43]. Moreover, the degradation that occurred after reaching 335 °C was a consequence of the pyrolysis reaction [44]. On the other hand, the TGA thermograms of the prepared CMC cryogels obtained with DVS crosslinking at 2.5, 20, and 100% showed similar thermal degradation profiles with the CMC, but the thermal stabilities decreased slightly and depended on the degree of the crosslinker ratio [39]. TGA thermograms of CMC-based cryogels and the corresponding TA composites were also compared in Figure 2b. The CMC 100% X cryogels degraded in one step in the 260–320 °C range with a 49.6% weight loss. On the other hand, the TA including composites of CMC cryogels started to degrade at lower temperatures than bare CMC cryogels. The weight loss values for TA@CMC 10% and TA@CMC 25% cryogel composites were determined as 25.9 and 33.7% in the 230–270 °C range. It was observed that the higher TA content provides higher degradation amounts at the same temperature ranges.

The elemental analyses of CMC-based cryogels and their TA-containing composites were carried out to corroborate the success of the crosslinking of CMC with DVS. The theoretical calculations and the elemental analysis results of C, H, and S% of CMC-based cryogels prepared at various crosslinking ratios were summarized in Table 1. It was seen that all theoretically calculated and elemental analysis results for the determined C, H, and O+Na% elements of CMC molecules are very similar. However, the theoretically calculated

C, H, and O+Na% ingredients of CMC-based cryogels are completely different than the results of the elemental analysis for all cryogels. First, the most outstanding difference and evidence of cryogel network synthesis by DVS crosslinking is the content of S% stemming from the used crosslinker, DVS. Accordingly, the S% amounts, as expected, are increased as the amount of used DVS is increased, e.g., as 10, 25, 50, and 100% per mole DVS, based on the repeating unit of CMC, are used, the S% amounts were determined as 0.68, 1.63, 3.07, and 5.52%, respectively, for the theoretical calculations.

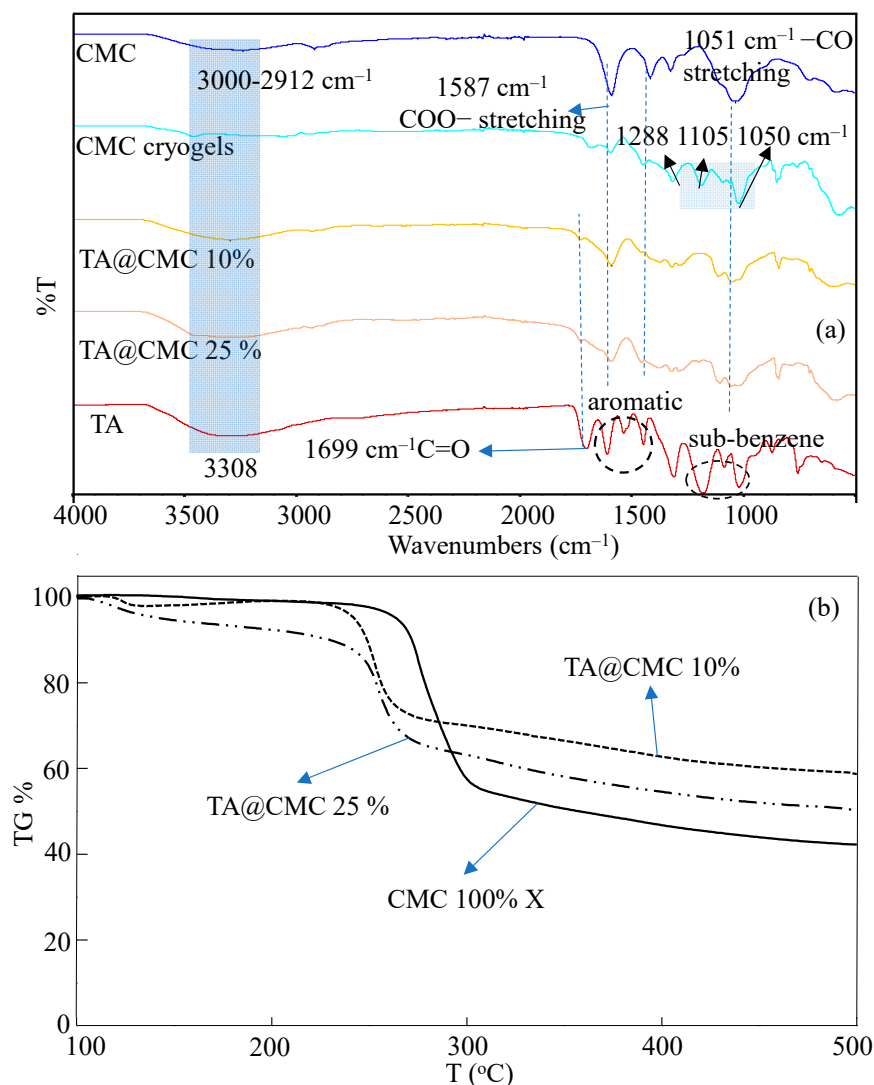


**Figure 2.** (a) FT-IR spectrum and (b) TGA thermograms of CMC, TA@CMC 10%, and TA@CMC 25% cryogels.

**Table 1.** The elemental composition of prepared CMC-based cryogels.

Materials	Theoretical				Elemental Analysis			
	C%	H%	S%	O+Na%	C%	H%	S%	O+Na%
CMC	46.7	4.76	-	48.48	45.3	4.97	-	49.73
CMC 10% X	46.6	4.77	0.68	47.95	35.9	5.25	0.97	57.88
CMC 25% X	46.4	4.78	1.63	47.19	35.6	5.25	1.00	58.15
CMC 50% X	46.1	4.79	3.07	46.04	35.2	5.27	1.04	58.49
CMC 100% X	45.5	4.83	5.52	44.15	34.8	5.15	1.30	58.75
TA@CMC 10%	46.1	4.72	5.11	44.08	30.4	4.48	1.06	64.06
TA@CMC 25%	46.9	4.52	4.60	43.98	30.7	4.29	0.95	64.06

On the other hand, the S% values for the 10, 25, 50, and 100% crosslinked CMC cryogels were determined as 0.97, 1.00, 1.04, and 1.30%, respectively, via elemental analysis. Based on these results, it is apparent that the CMC-based cryogels, which were theoretically thought to be 10, 25, 50, and 100% crosslinked, were actually crosslinked as 14.3, 15.4, 16.9, and 23.5% based on the CMC repeating unit, respectively, via the elemental analysis results. On the other hand, the theoretically calculated S% values for the 10 and 25% *w/w* TA-containing TA@CMC cryogel composites were calculated as 5.11 and 4.60, respectively, whereas these values were experimentally determined as 1.06 and 0.95%, respectively. It was understood that the TA molecule decreases the crosslinking extent as compared to the cryogel prepared at the same crosslinking ratio of DVS without TA. It is reasonable as the TA molecule increases the pH of cryogel precursors, leading to a decrease in the extent of the crosslinking reaction, which occurs by the Michael-addition reaction that requires basic pH media. Moreover, the higher differences between the O+Na% values that were theoretically calculated and experimentally determined can be related to the use of NaOH solution to dissolve CMC and TA before the crosslinking reaction.

The digital camera images of both CMC and TA@CMC cryogels at dry and swollen states are given in Figure 3a. It is clearly seen that the color of cryogels turned brownish with the presence of TA in the CMC cryogels. On the other hand, the SEM images of the prepared CMC-based cryogels were also taken to prove interconnected super porous structures of cryogels. The SEM images in Figure 3b show the super porous structure of CMC-based cryogels that are affected by the presence of TA as the pores were smaller. Pore walls can be realized in both the SEM images and the microscope images provided in Figure S1. To assess the effect of TA amount in CMC cryogels on pore sizes and pore size distribution% for CMC, TA@CMC 10%, and TA@CMC 25% cryogels, ImageJ software version 1.8.0. [45] was applied to a randomly selected 30 pores in the corresponding SEM images. The calculated average pore sizes were given in Figure 3d and determined as  $182 \pm 89 \mu\text{m}$  for CMC cryogels, which decreased to  $165 \pm 89$  and  $98 \pm 64 \mu\text{m}$  for TA@CMC 10% and TA@CMC 25% cryogels, respectively. The pore size distribution% of CMC, TA@CMC 10%, and TA@CMC 25% cryogels was also compared and presented in Figure 3d. It was clearly seen that all cryogels have pores in their super pore range, and the size distribution for higher TA content is reduced. However, the CMC cryogels possess 33.3% pores in range of 200–300  $\mu\text{m}$ , whereas most of the pores of TA@CMC 10% cryogels are in the range of 200–100  $\mu\text{m}$  (almost 45%). On the other hand, as the pore size distribution of TA@CMC 25% cryogels was examined, it was determined that more than 90% of the pores were smaller than 200  $\mu\text{m}$ . Consequently, it is obvious that CMC-based cryogels with their open pore walls are intriguing biomaterials for potential use in tissue engineering with tunable porosity for the proliferation of cells and/or for the separation of different cells for different purposes.

As the cryogels possess an interconnected super porous structure, they afford significant advantages in biomedical applications. The parameters such as swelling%, porosity%, and pore volume (mL/g) are very important and need to be determined. Therefore, all these parameters for the CMC-based cryogels prepared by using various crosslinker ratios were determined, and the corresponding results are summarized in Table 2. It is obvious that, by the increase in the amount of crosslinking ratio from 10 to 100%, the swelling ability of CMC-based cryogels decreased from  $2247 \pm 92$  to  $1659 \pm 95\%$ . This is reasonable and expected by the fact that highly crosslinked CMC chains are connected to each other more tightly with the increase in the crosslinker ratio, resulting in swelling to a lesser degree. Moreover, the P% values calculated for CMC-based cryogels increased from  $47.4 \pm 1.9$  to  $67.9 \pm 1.2\%$  with the increased amount of the crosslinking ratio from 10 to 100%. On the other hand, the V<sub>p</sub> values decreased from  $18.4 \pm 0.9$  to  $10.5 \pm 0.8 \text{ mL/g}$  with the increasing degree of the crosslinking ratio. These all make sense; as the crosslink density of the cryogel network increases with the increased amount of crosslinker, the degree of swelling decreases and the crosslink density of the cryogel network increases. It is also evident that as the DVS content increases, the porosity (P%) is also increased due to the relatively more rigid pore generation.



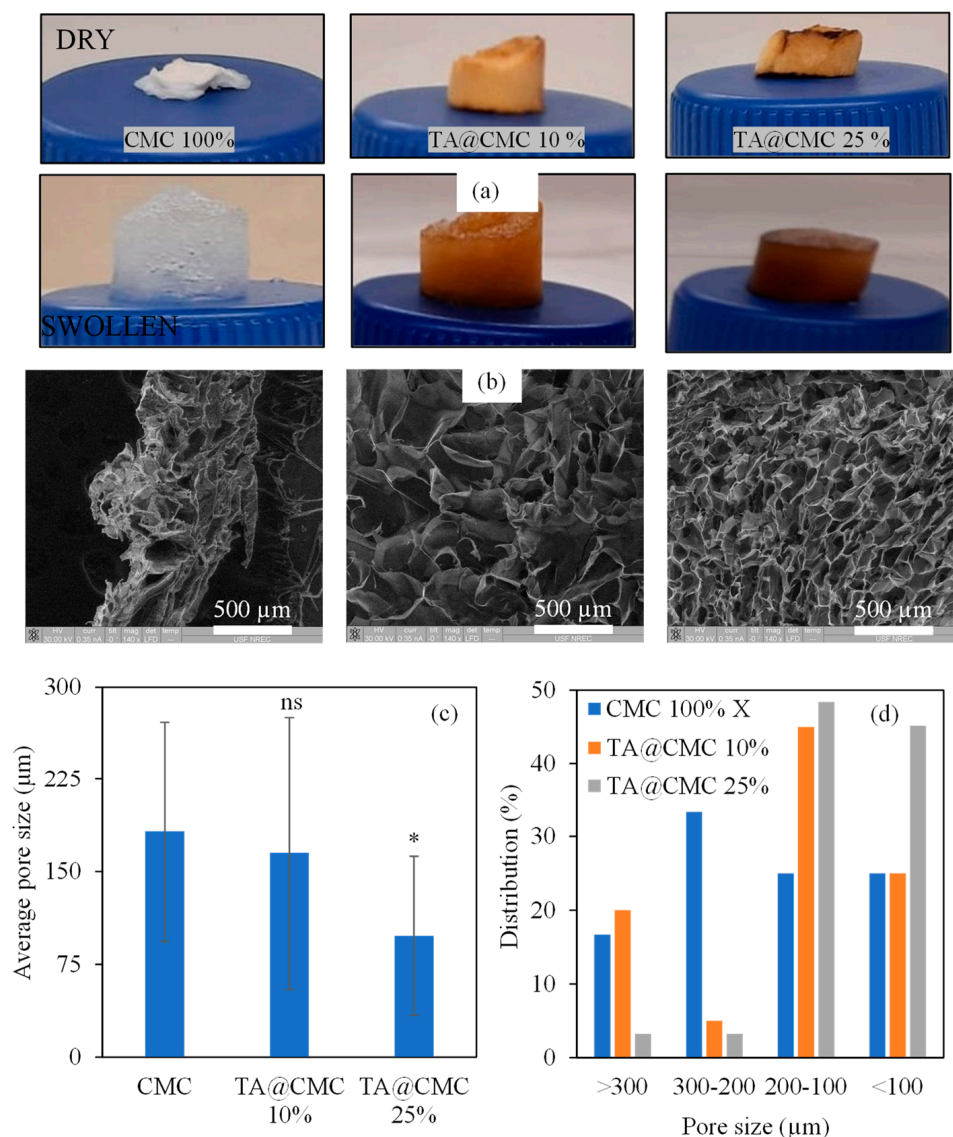


**Figure 3.** (a) Dry and water-swollen CMC, TA@CMC 10%, and TA@CMC 25% cryogels, (b) their corresponding SEM images, and (c) their average pore sizes, and (d) pore size distribution% comparison of CMC-based cryogels. ns: non-significant, \*  $p < 0.05$  compared with CMC cryogel as control group.

**Table 2.** The swelling% (S%), porosity% (P%), pore volume ( $V_p$ ), and gel yield% values for prepared CMC-based cryogels.

Cryogels	S%	P%	$V_p$ (mL/g)	Gel Yield%
CMC 10% X	2247 ± 92	47.4 ± 1.9	18.4 ± 0.9	74.1 ± 1.8
CMC 25% X	2174 ± 95	57.3 ± 1.4	14.6 ± 0.8	82.5 ± 2.1
CMC 50% X	2145 ± 91	60.8 ± 1.4	12.9 ± 0.9	94.1 ± 1.7
CMC 100% X	1659 ± 95	67.9 ± 1.2	10.5 ± 0.8	94.9 ± 0.9

The gel yield% values were also calculated for the prepared CMC-based cryogels, and, as anticipated, the gel yield% increased from  $74.1 \pm 1.8$  to  $94.9 \pm 0.9\%$  with the increase in the amount of used crosslinker ratio from 10 to 100%.

### 3.2. Degradability of Prepared CMC-Based Cryogels

The degradability of polymers/hydrogels is another important parameter that affects the potential biomedical applications [46–48]. The intrinsic degradability of the biomolecule-

derived crosslinked structures by enzymes, oxidative stress, and pH-sensitive environments in the body need to be taken into consideration. As a result, the hydrolytic breakdown of the cryogels based on CMC was studied at several pH solution values, 1.0, 7.4, and 9.0. These solution pHs were chosen due to their fit for multiple human systems and/or organs, such as the stomach, blood, intestinal pH, endosomal/lysosomal environment, and so on [49–51]. The hydrolytic degradation profiles of all CMC-based cryogels crosslinked with 10, 25, 50, and 100% crosslinking ratios at pHs 1.0, 7.4, and 9.0 are compared and shown Figure 4a, b, and c, respectively. The hydrolytic degradation profiles of CMC-based cryogels at pH 1.0 are given in Figure 4a. A higher degradation% was observed for CMC 10% cryogels; as  $27.5 \pm 1.6\%$  of CMC 10% cryogels was degraded in 3 days and degradation increased slightly,  $28.3 \pm 1.2\%$  degradation was observed up to 7 days. On the other hand,  $19.6 \pm 1.3$ ,  $14.1 \pm 1.0$ , and  $11.8 \pm 1.00\%$  of CMC cryogels were degraded, which were crosslinked at 25, 50, and 100%, respectively, in pH 1.0 at the end of 7 days.

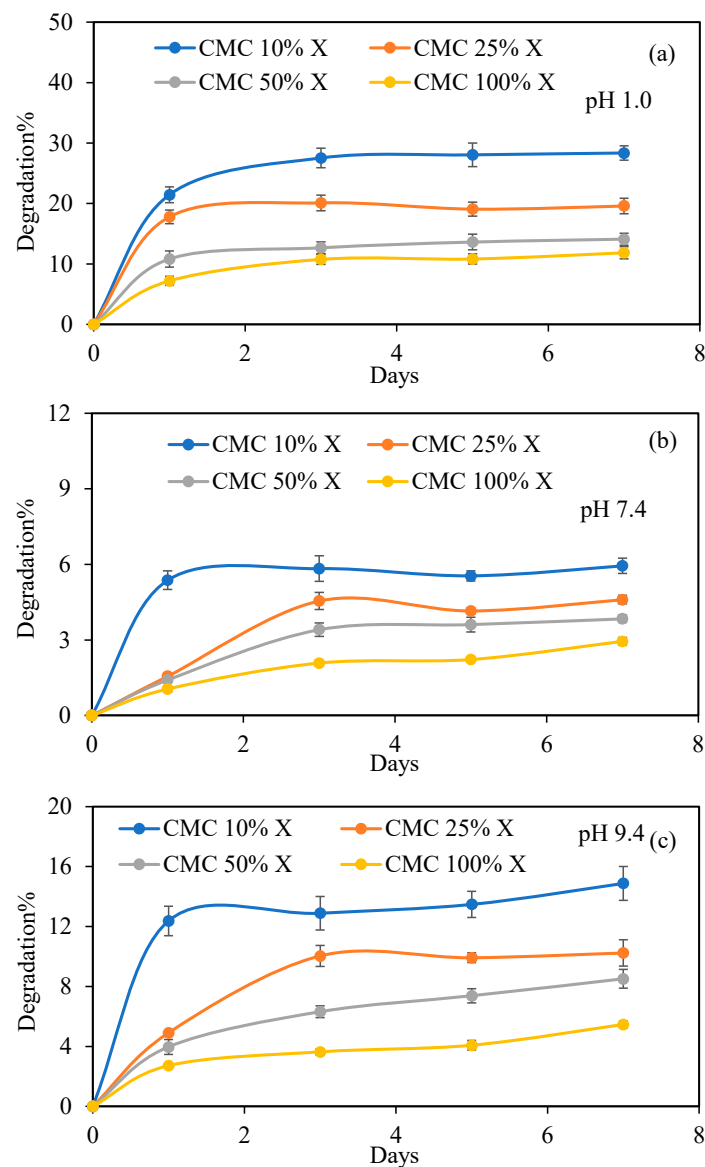


**Figure 4.** Comparison of hydrolytic degradation of CMC-based cryogels at pH (a) 1.0, (b) 7.4, and (c) 9.0 buffer solutions.

The same degradation profiles, to a lesser degree, were also observed for CMC-based cryogels at pH 7.4 in 7 days, and the corresponding graph is given in Figure 4b. As expected, a slightly higher degradation% was observed for CMC 10% cryogels,  $5.9 \pm 0.3\%$  in 7 days

at pH 7.4, in comparison to the degradation% for CMC-based 25, 50, and 100% cryogels, which were degraded as  $4.6 \pm 0.2$ ,  $3.8 \pm 0.2$ , and  $2.9 \pm 0.2\%$ , respectively. The hydrolytic degradation% values for CMC cryogels prepared at 10, 25, 50, and 100% crosslinking ratios at pH 9.0 in 7 days were determined as  $14.9 \pm 1.1$ ,  $10.2 \pm 0.8$ ,  $8.5 \pm 0.6$ , and  $5.5 \pm 0.2\%$ , respectively, as shown in Figure 4c. In summary, it can be concluded that the crosslinking ratio can directly affect the degradability of CMC-based cryogels as the lower crosslinking ratio, the higher the degradability of CMC-based cryogels. Additionally, the extent of degradation% depends on the pH of the medium as CMC-based cryogels show different degradability% at different pH values, and the degradation extent of CMS cryogels is  $\text{pH } 1.0 > \text{pH } 9.0 > \text{pH } 7.4$ .

### 3.3. TA-Release Ability of CMC Cryogels

Materials containing TA are becoming more prevalent in biomedical and pharmaceutical applications because of their potent anti-inflammatory, antibacterial, antioxidant, and even anticancer properties. Thus, TA@CMC cryogel composites can be used as drug carrier and delivery systems, e.g., as a TA-release system or for the release of different bioactive molecules or drugs. The pH of various human body environments varies; for example, the physiological pH of blood plasma is 7.4, the pH of the pancreas and intestinal tract is approximately 9.0, and the pH of the stomach is approximately 1.0. To illustrate the potential biological use of TA@CMC containing 10 and 25% TA, the TA-release studies were conducted at these three different pH environments: pH 1.0, pH 7.4, and pH 9.0. The TA@CMC cryogel samples were removed from the release medium at predetermined intervals, and TA released up to 480 min utilizing UV-Vis spectroscopy was determined. In Figure 5a,b, the TA-release profile from each TA@CMC 10% and 25% cryogel matrix, respectively, for different pH buffer solutions is illustrated.

In Figure 5a, the amount of released TA from TA@CMC 10% cryogels is linearly increased up to 120 min with  $22.9 \pm 1.3$  mg TA/g and continued to  $23.6 \pm 1.1$  mg TA/g release in 480 min at pH 7.4. On the other hand, the released amount of TA from TA@CMC 10% cryogels is also linear up to 120 min, and 60 min, with the released amounts of  $14.5 \pm 0.3$  and  $8.3 \pm 0.1$  mg TA/g at pH 1 and 9, respectively. And up to 480 min, the TA released amounts were determined as  $14.7 \pm 0.4$  and  $8.7 \pm 0.1$  mg TA/g at pH 1.0 and 9.0, respectively. On the other hand, the TA release from TA@CMC 25% cryogels was also investigated at pH 1.0, 7.4, and 9.0, and the corresponding graph is given in Figure 5b. It was seen that  $34.0 \pm 2.9$  mg TA/g was released at pH 7.4 in 15 min, and TA release was slowly continued up to 480 min with a total  $46.5 \pm 2.2$  mg TA/g. The TA release from TA@CMC 25% cryogels at pH 1.0 was calculated as  $14.1 \pm 1.2$  mg TA/g in 5 min and slowly continued up to  $29.8 \pm 2.1$  mg TA/g release in 480 min. The lower TA release from TA@CMC 25% cryogels was observed at pH 9.0 with  $16.5 \pm 1.1$  mg TA/g in 60 min and  $16.9 \pm 1.1$  mg TA/g in 480 min. The released TA% from TA@CMC cryogels at pHs 1.0, 7.4, and 9.0 in 480 min was also compared, and the results were summarized in Figure 5c. The amounts of TA within the TA@CMC 10 and 25% cryogel were assumed to be 100 mg TA/g and 250 mg TA/g, according to the weight ratio of CMC and TA during the synthesis process. In this context, the amounts of released% of TA from TA@CMC 10% cryogels at pH 1.0, 7.4, and 9.0 were calculated as  $14.7 \pm 0.4$ ,  $23.6 \pm 1.1$ , and  $8.7 \pm 0.1\%$ , respectively. On the other hand, the release% values of TA from TA@CMC 25% cryogels at pH 1.0, 7.4, and 9.0 were calculated as  $11.9 \pm 0.8$ ,  $18.6 \pm 0.9$ , and  $6.7 \pm 0.4\%$ , respectively. In neutral conditions, as opposed to acidic and basic environments, the TA@CMC cryogels can release higher amounts of TA. As a result, as Figure 5 illustrates, the release rates of the total released amounts of TA can be controlled depending on the medium's pH and on the amounts of TA used during the cryogel composites synthesis. As expected, the amount and rate of TA release rose as the amount of TA in the cryogel composites increased. This offers a significant advantage to the design and controlled-release systems not just for an antioxidant compound such as TA but also some other bioactive molecules such as drugs, peptides, enzymes, growth factors, and so on.

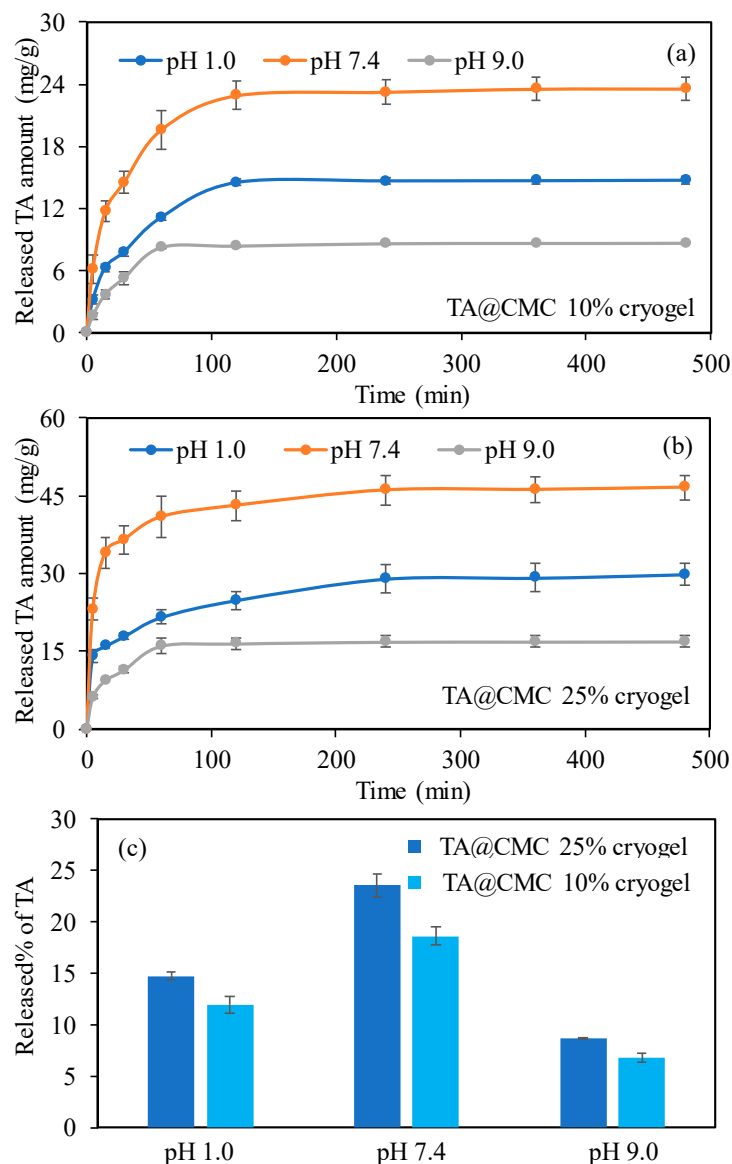


**Figure 5.** The TA-release profiles of (a) TA@CMC 10%, (b) TA@CMC 25% cryogels, and (c) released % of TA from TA@CMC 10% and 25% cryogels at pH 1.0, 7.4, and 9.0 at the end of 480 min.

In Figure 6, the antioxidative capacities of TA@CMC cryogels were tested at varying concentrations according to four different antioxidant tests. In Figure 6a, the total phenol content of CMC cryogels at 2000  $\mu\text{g}/\text{mL}$  is determined as  $9.3 \pm 0.7$ , while for TA@CMC 10% and TA@CMC 25%, the total phenol contents, determined as  $26.4 \pm 2.8$  and for  $39.8 \pm 0.5$   $\mu\text{g}/\text{mL}$  GA eq, respectively, are obtained at the same concentration. The total phenol content increases depending on the TA concentration. Figure 6b shows the total flavonoid content (TFC) according to rosmarinic acid equivalency where CMC cryogels have no antioxidant value. On the other hand, TA@CMC cryogels have a TFC dependency based on the TA content. At a concentration of 2000  $\mu\text{g}/\text{mL}$ , TA@CMC 25% was determined by a TFC value of  $23.4 \pm 10.5$   $\mu\text{g}/\text{mL}$  RA eq, whereas TA@CMC 10% was administered at  $9.2 \pm 1.5$   $\mu\text{g}/\text{mL}$  RA eq at the same concentration.

In Figure 6c, the Fe(III) reduction capacity data of CMC-based cryogels are given. While CMC cryogel did not reduce Fe ions, the TA@CMC 25% and TA@CMC 25% cryogels were found to reduce  $56.2 \pm 3.2$   $\mu\text{mol}$   $37.94 \pm 5.8$  Fe(III), respectively, at 2000  $\mu\text{g}/\text{mL}$  concentration. The Fe(II) chelation capacities of CMC materials are shown in Figure 6d. It is apparent that the CMC cryogels can chelate with Fe(II) ions with a concentration-dependent profile. Similarly, TA-containing cryogels also can chelate with Fe(II) ions

via a concentration-dependent manner; CMC cryogels exhibited  $59.2 \pm 3.3\%$  chelation at a concentration of  $125 \mu\text{g/mL}$ , while the TA@CMC 10% and TA@CMC 2% cleated a  $66.9 \pm 2.1\%$  and  $55.3 \pm 1.8\%$  chelate with an Fe(II) ion chelating ability at the same concentrations. It is obvious from Figure 6d that TA and CMC has similar Fe(II) ion binding capabilities with competitive binding abilities due to their abundant number of -OH and -COOH functional groups.

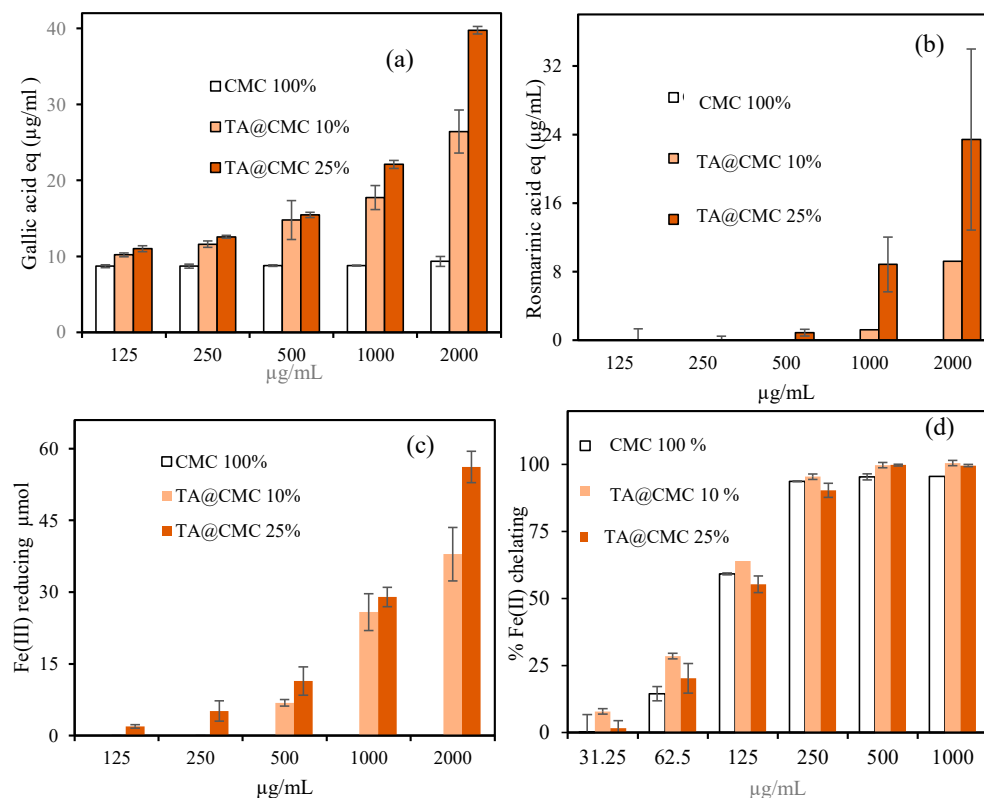


**Figure 6.** (a) Total phenol, (b) total flavonoid content, (c) Fe(III) ion reducing, and (d) Fe(II) chelating activity of CMC and TA@CMC-based cryogels.

### 3.4. Blood Compatibility of CMC-Based Cryogels

The blood compatibility of materials is of great value in biomedical applications [52–54]. The interactions of materials with blood need to be tested to assess the use of these materials in blood-contacting application. Commonly, the two-test hemolysis%, which is a measure of the red blood cell rupture capacity of the materials and the blood-clotting index% assay, which measure the effect on the blood coagulation mechanism of the materials are used to determine the blood compatibility of the materials [31,55]. Here, the hemolysis% values of  $1 \text{ mg/mL}$  concentrations of CMC-based cryogels were measured and compared in the results shown in Figure 7a. It is clearly seen that, with the increase in the crosslinking ratio from the 10 to 100% weigh ratio of CMC, there is a slight increase in the hemolysis% of CMC-based cryogels, e.g., from  $0.21 \pm 0.03$  to  $0.82 \pm 0.21\%$ , respectively. However, this increase is not important, and all CMC-based cryogels in the 10–100% crosslinked ratio are non-hemolytic as a  $<5\%$  hemolysis ratio is defined as non-hemolytic [56]. On the other hand, the hemolysis% values were determined as  $2.7 \pm 0.9$  and  $6.1 \pm 0.8\%$  at a  $1.0 \text{ mg/mL}$  concentration of TA@CMC 10% and 25% cryogels, respectively. This means that the presence of TA within CMC cryogels affected the non-hemolytic nature of CMC cryogels, and the increase in the amount of TA in TA@CMC cryogels makes CMC-based cryogels slightly hemolytic at TA  $> 25 \text{ mg}$  or capable of damaging the erythrocyte cells. It has already been reported in the literature that TA can destroy erythrocyte cells depending

on their amount, resulting in hemolysis [31], yet  $\leq 25$  mg TA per gram of CMC cryogels can be considered non-hemolytic.

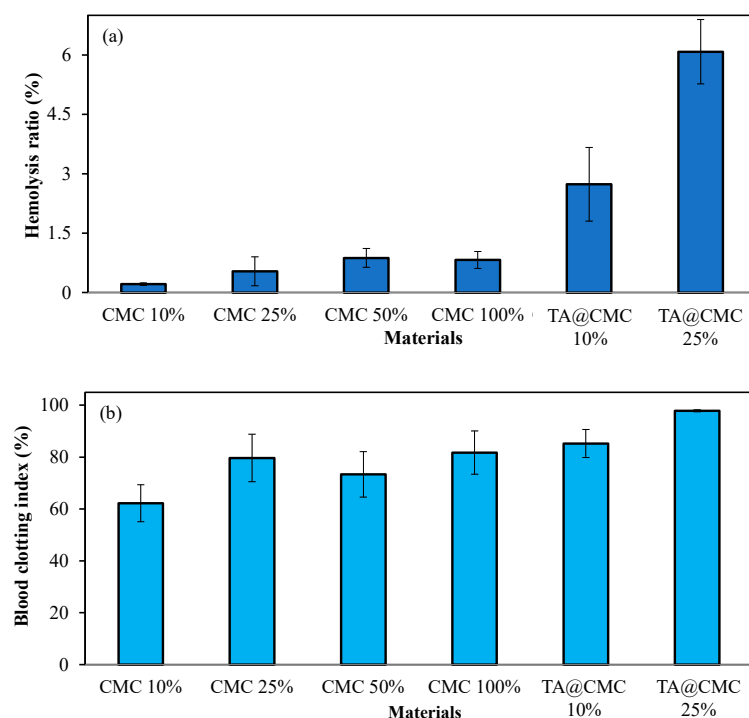


**Figure 7.** Blood compatibility of CMC-based cryogels based on (a) hemolysis %, and (b) blood clotting index (%) at test.

Another test, the blood-clotting index (BCI) is a commonly used technique to assess a material's blood compatibility. Depending on the requirements, e.g., even sometimes excess bleeding, clotting the blood may be required to stop the loss of the blood or may also be useful for wound-dressing materials. However, in general, there should be no interference with the blood-clotting mechanisms for the materials' use in biomedical applications. Therefore, the BCI at about 100% assumed no inference with the blood. As shown in Figure 7b, the BCI values for CMC-based cryogels crosslinked at various amounts of crosslinkers, 10–100%, revealed BCI values of  $62.1 \pm 7.1$ – $81.7 \pm 8.3\%$ , which affect the blood coagulation mechanism at 1.0 mg/mL concentrations. It is obvious that the increase in the amount of the crosslinker DVS decreases the BCI values of CMC-based cryogels. It was reported that the formation of hard clots was promoted in the presence of CMC, which indicates that CMC does not start the initiation of the clotting mechanism but accelerated clotting developments [55]. Interestingly, as CMC cryogels contain certain amounts of TA, e.g., TA@CMC cryogels containing 10% and 25% of TA, higher BCI values were afforded, namely,  $85.2 \pm 5.4$  and  $97.8 \pm 0.4\%$ , respectively. Although, several studies had been reported about the coagulative effect of tannic acid [2,23], the prepared TA@CMC cryogels exhibited less coagulative properties than bare CMC cryogels at 1 mg/mL concentrations. This can be due to the decreasing amount of CMC and the amount of TA in TA@CMC cryogels (10% and 25% TA content of cryogel), and the TA and CMC may have different coagulation mechanisms in the blood. It was reported that the blood coagulation mechanism is not effected for TA concentrations at  $\leq 0.01$  mg/mL [31]. Therefore, the increased amount of TA in TA@CMC cryogels provides higher BCI values.

### 3.5. Antibacterial and Enzyme Inhibition Capabilities of CMC-Based Cryogels

To further evaluate the potential usability of TA@CMC cryogels in biomedical applications, their antimicrobial abilities were tested against a Gram-negative bacterium, *E. coli*, and a Gram-positive bacterium, *S. aureus*. *E. coli* is widespread in the environment, easily

transmitted through the fecal–oral route, and associated with serious illnesses such as bacteremia, sepsis, inflammatory bowel disease, urinary tract infections, and diarrhea [57]. *S. aureus* is also common in public places such as schools, hospitals, etc., and causes infections of the osteoarticular system, eye, skin, soft tissue, and implants [58,59]. Upon a 24 h incubation of the CMC cryogels and TA@CMC cryogels with these pathogens, Table 2 summarizes the results after inoculating CMC cryogels and TA@CMC cryogels on nutrient broth and nutrient agar. As given in Table 3, the minimum inhibition concentration (MIC) for TA@CMC 25% cryogel is 5 mg/mL against *E. coli* bacteria, whereas the CMC cryogels have no MIC values against both microorganisms.

**Table 3.** MIC and MBC values of TA@CMC cryogels against *E. coli* and *S. aureus*.

Material	<i>E. coli</i>		<i>S. aureus</i>	
	MIC (mg/mL)	MBC (mg/mL)	MIC (mg/mL)	MBC (mg/mL)
TA@CMC 25%	5	-	10	-
CMC 100X	-	-	-	-

$\alpha$ -glucosidase is one of the hydrolytic enzymes that break down disaccharides' bonds, and  $\alpha$ -glucosidase inhibitors are used for type 2 diabetes. The enzyme inhibition of CMC-based cryogels is shown in Figure 8a. The CMC cryogels did not show any inhibitory effect on the enzyme; on the other hand, the TA@CMC cryogels inhibited  $\alpha$ -glucosidase enzyme in a concentration-dependent manner. At a concentration of 1500  $\mu$ g/mL, TA@CMC 10% inhibited the cryogel by  $36.5 \pm 6.5\%$ , whereas the TA@CMC 25% inhibited it by  $57.9 \pm 2.4\%$  at the same concentration and, upon increasing its concentration to 3000  $\mu$ g/mL, the enzyme inhibition capacities are increased to  $43.6 \pm 3.8\%$  and  $71.6 \pm 2.4\%$ , whereas CMC had only  $6.5 \pm 0.2\%$   $\alpha$ -glucosidase inhibition capacity.

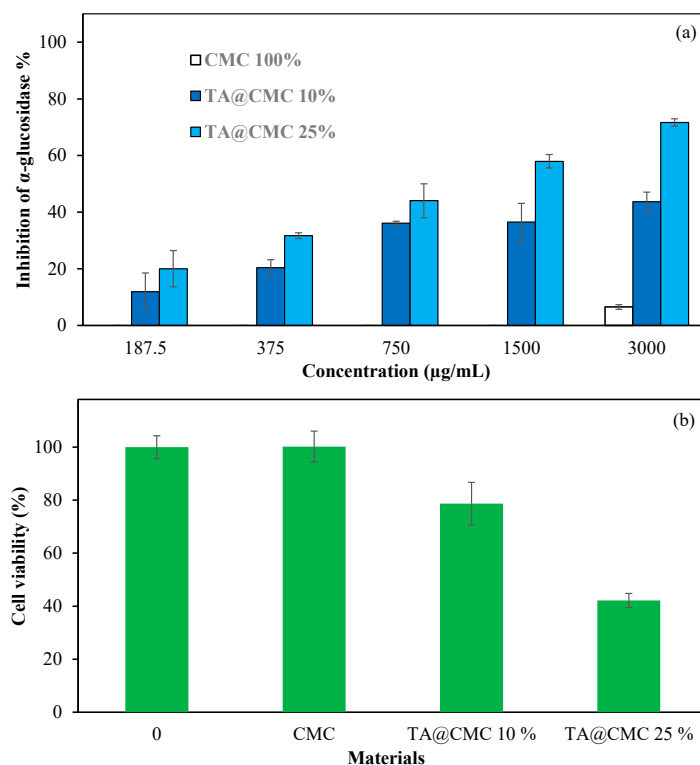


**Figure 8.** (a) Inhibition of  $\alpha$ -glucosidase of CMC and TA@CMC cryogels and (b) their cell viability against L929 fibroblast cell lines.

The biocompatibility results for 1 mg weight of CMC-based cryogel are shown in Figure 8b. As can be seen, CMC 100% cryogels showed the highest biocompatibility, with  $100.2 \pm 5.8\%$  cell viability. On the other hand, the cryogels with TA demonstrated less cell viability, and their biocompatibility is reduced with the increase in the amount of TA as TA@CMC 10% and TA@CMC 25% showed cell viability of  $78.7 \pm 8.0\%$  and  $42.1 \pm 2.6\%$ , respectively.

#### 4. Conclusions

Here, the synthesis of CMC with different amounts of crosslinkers, 10–100%, in presence of a natural polyphenolic, TA (as TA@CMC cryogels with interconnected super porous network structures) was successfully prepared under cryogenic conditions. As expected, the swelling ability of CMC-based cryogels decreased from 2250 to 1650% by changing the amount of the crosslinker DVS from 10% to 100% based on the repeating unit of CMC. Also, as anticipated, higher hydrolytic degradation was obtained for 10% crosslinked CMC cryogels at all pH values, 1.0, 7.4, and 9.0; amongst these pHs, the highest hydrolytic degradation was observed at pH 1.0 for all CMC 10% X cryogels. Furthermore, the TA-release profiles of TA@CMC 10% and 25% cryogels showed that about 25% TA content of TA@CMC 10% cryogels and 20% of TA content of TA@CMC 25% cryogel at pH 7.4 were released in 480 min. All CMC-based cryogels were found to be non-hemolytic with a hemolysis ratio of 1% at a concentration of 1.0 mg/mL. However, the TA@CMC 25% cryogels with a hemolysis ratio of  $6.1 \pm 0.8\%$  were found to be slightly hemolytic, whereas TA@CMC 10% cryogels with a hemolysis ratio of  $<3\%$  at concentrations of 1.0 mg/mL were determined as non-hemolytic. The BCI index values for CMC-based cryogels ranged from 62 to 82% in the crosslinking range of 10–100% for CMC cryogels, suggesting that CMC cryogels can affect the blood-clotting mechanism. On the other hand, the BCI value for TA@CMC 25% cryogels was found to be  $97.8 \pm 0.4\%$ , which means that it does not affect the blood-clotting mechanism. Furthermore, CMC cryogels at different % crosslinking ratios show no MIC values, whereas TA@CMC 25% has MIC values of 5 and 10 mg/mL against *E. coli* and *S. aureus*, respectively. Additionally, CMC cryogel at different% crosslinking ratios has minimal  $\alpha$ -glucosidase enzyme inhibition ability, e.g., events at 3000  $\mu\text{g/mL}$  concentration had  $6.5 \pm 0.2\%$   $\alpha$ -glucosidase inhibition capacity, whereas TA@CMC 10% and TA@CMC 25% had concentration-dependent enzyme inhibition ability. At 3000  $\mu\text{g/mL}$  concentration, the TA@CMC 10% and TA@CMC 25% cryogels inhibited the  $43.6 \pm 3.8\%$  and  $71.6 \pm 2.4\%$  of  $\alpha$ -glucosidase enzymes. Finally, the CMC cryogels have no toxicity on fibroblast cells, while TA@CMC 10% and TA@CMC 25% cryogels showed reduced cell viability with the increased amount of TA content, e.g.,  $78.7 \pm 8.0\%$  and  $42.1 \pm 2.6\%$ , respectively, observed for both TA-containing cryogels. Therefore, CMC cryogel with TA-containing forms can be readily tuned to obtain their combined natural properties such as blood compatibility, antioxidant, antibacterial, and  $\alpha$ -glucosidase enzyme inhibition abilities for different biomedical uses.

**Supplementary Materials:** The following supporting information can be downloaded at <https://www.mdpi.com/article/10.3390/polysaccharides5040051/s1>. Supporting Information Figure S1: The microscope images of CMC-based cryogels.

**Author Contributions:** Conceptualization, M.S. and N.S.; methodology, M.S. and S.D.; software, M.S. and S.D.; validation, M.S., S.D. and N.S.; formal analysis, M.S.; investigation, M.S. and S.D.; resources, N.S.; data curation, M.S., S.D. and N.S.; writing—original draft, M.S. and S.D.; writing—review and editing, N.S.; visualization, M.S. and N.S.; supervision, N.S.; project administration, N.S.; funding acquisition, N.S. All authors have read and agreed to the published version of the manuscript.

**Funding:** This research received no external funding.

**Institutional Review Board Statement:** Human blood was collected from healthy volunteers for blood analysis with the approval of Canakkale Onsekiz Mart University, Human Research Ethics Committee (2011-KAEK-27/2022).



**Data Availability Statement:** No new data were generated or externally used in this research.

**Acknowledgments:** The authors thank Selin S. Suner for cytotoxicity studies and Betül Ari for the blood compatibility studies.

**Conflicts of Interest:** The authors declare no conflicts of interest.

## References

- Bakhshpour, M.; Idil, N.; Perçin, I.; Denizli, A. Biomedical Applications of Polymeric Cryogels. *Appl. Sci.* **2019**, *9*, 553. [[CrossRef](#)]
- Tyshkunova, I.V.; Poshina, D.N.; Skorik, Y.A. Cellulose Cryogels as Promising Materials for Biomedical Applications. *Int. J. Mol. Sci.* **2022**, *23*, 2037. [[CrossRef](#)] [[PubMed](#)]
- Eggermont, L.J.; Rogers, Z.J.; Colombani, T.; Memic, A.; Bencherif, S.A. Injectable Cryogels for Biomedical Applications. *Trends Biotechnol.* **2020**, *38*, 418–431. [[CrossRef](#)] [[PubMed](#)]
- Çimen, D.; Özbek, M.A.; Bereli, N.; Mattiasson, B.; Denizli, A. Injectable Cryogels in Biomedicine. *Gels* **2021**, *7*, 38. [[CrossRef](#)]
- Memic, A.; Colombani, T.; Eggermont, L.J.; Rezaeeyazdi, M.; Steingold, J.; Rogers, Z.J.; Navare, K.J.; Mohammed, H.S.; Bencherif, S.A. Latest Advances in Cryogel Technology for Biomedical Applications. *Adv. Ther.* **2019**, *2*, 1800114. [[CrossRef](#)]
- Orakdogan, N.; Karacan, P.; Okay, O. Macroporous, responsive DNA cryogel beads. *React. Funct. Polym.* **2011**, *71*, 782–790. [[CrossRef](#)]
- Mu, Y.; Wang, X.; Du, X.; He, P.-P.; Guo, W. DNA Cryogels with Anisotropic Mechanical and Responsive Properties for Specific Cell Capture and Release. *J. Am. Chem. Soc.* **2024**, *146*, 5998–6005. [[CrossRef](#)]
- Wan, W.; Bannerman, A.D.; Yang, L.; Mak, H. Poly(Vinyl Alcohol) Cryogels for Biomedical Applications. In *Polymeric Cryogels*; Okay, O., Ed.; Springer: Cham, Switzerland, 2014; pp. 283–321.
- Ari, B.; Sahiner, M.; Demirci, S.; Sahiner, N. Poly(vinyl alcohol)-tannic Acid Cryogel Matrix as Antioxidant and Antibacterial Material. *Polymers* **2021**, *14*, 70. [[CrossRef](#)]
- Razavi, M.; Qiao, Y.; Thakor, A.S. Three-dimensional cryogels for biomedical applications. *J. Biomed. Mater. Res. Part A* **2019**, *107*, 2736–2755. [[CrossRef](#)]
- Ceylan, S.; Göktürk, D.; Bölgen, N. Effect of crosslinking methods on the structure and biocompatibility of polyvinyl alcohol/gelatin cryogels. *Bio-Med. Mater. Eng.* **2016**, *27*, 327–340. [[CrossRef](#)]
- Omidian, H.; Dey Chowdhury, S.; Babanejad, N. Cryogels: Advancing Biomaterials for Transformative Biomedical Applications. *Pharmaceutics* **2023**, *15*, 1836. [[CrossRef](#)] [[PubMed](#)]
- Savina, I.N.; Zoughaib, M.; Yergeshov, A.A. Design and Assessment of Biodegradable Macroporous Cryogels as Advanced Tissue Engineering and Drug Carrying Materials. *Gels* **2021**, *7*, 79. [[CrossRef](#)] [[PubMed](#)]
- Mendes, B.B.; Gómez-Florit, M.; Araújo, A.C.; Prada, J.; Babo, P.S.; Domingues, R.M.A.; Reis, R.L.; Gomes, M.E. Intrinsically Bioactive Cryogels Based on Platelet Lysate Nanocomposites for Hemostasis Applications. *Biomacromolecules* **2020**, *21*, 3678–3692. [[CrossRef](#)] [[PubMed](#)]
- Rahman, M.S.; Hasan, M.S.; Nitai, A.S.; Nam, S.; Karmakar, A.K.; Ahsan, M.S.; Shiddiky, M.J.A.; Ahmed, M.B. Recent Developments of Carboxymethyl Cellulose. *Polymers* **2021**, *13*, 1345. [[CrossRef](#)] [[PubMed](#)]
- Saberi Riseh, R.; Gholizadeh Vazvani, M.; Hassanisaadi, M.; Skorik, Y.A. Micro-/Nano-Carboxymethyl Cellulose as a Promising Biopolymer with Prospects in the Agriculture Sector: A Review. *Polymers* **2023**, *15*, 440. [[CrossRef](#)]
- Seddiqi, H.; Oliaei, E.; Honarkar, H.; Jin, J.; Geonzon, L.C.; Bacabac, R.G.; Klein-Nulend, J. Cellulose and its derivatives: Towards biomedical applications. *Cellulose* **2021**, *28*, 1893–1931. [[CrossRef](#)]
- Tardy, B.L.; Mattos, B.D.; Otoni, C.G.; Beaumont, M.; Majoinen, J.; Kämäräinen, T.; Rojas, O.J. Deconstruction and Reassembly of Renewable Polymers and Biocolloids into Next Generation Structured Materials. *Chem. Rev.* **2021**, *121*, 14088–14188. [[CrossRef](#)]
- Cai, Z.; Wu, J.; Du, B.; Zhang, H. Impact of distribution of carboxymethyl substituents in the stabilizer of carboxymethyl cellulose on the stability of acidified milk drinks. *Food Hydrocoll.* **2018**, *76*, 150–157. [[CrossRef](#)]
- Yang, H.-R.; Li, S.-S.; An, Q.-D.; Zhai, S.-R.; Xiao, Z.-Y.; Zhang, L.-P. Facile transformation of carboxymethyl cellulose beads into hollow composites for dye adsorption. *Int. J. Biol. Macromol.* **2021**, *190*, 919–926. [[CrossRef](#)]
- Capanema, N.S.V.; Mansur, A.A.P.; de Jesus, A.C.; Carvalho, S.M.; de Oliveira, L.C.; Mansur, H.S. Superabsorbent crosslinked carboxymethyl cellulose-PEG hydrogels for potential wound dressing applications. *Int. J. Biol. Macromol.* **2018**, *106*, 1218–1234. [[CrossRef](#)]
- Kaczmarek, B. Tannic Acid with Antiviral and Antibacterial Activity as A Promising Component of Biomaterials—A Minireview. *Materials* **2020**, *13*, 3224. [[CrossRef](#)] [[PubMed](#)]
- Sahiner, N.; Sagbas, S.; Sahiner, M.; Silan, C. P(TA) macro-, micro-, nanoparticle-embedded super porous p(HEMA) cryogels as wound dressing material. *Mater. Sci. Eng. C* **2017**, *70*, 317–326. [[CrossRef](#)] [[PubMed](#)]
- Sasaki, Y.; Matsumoto, K.; Imanishi, H.; Watanabe, M.; Ohta, T.; Shirasu, Y.; Tutikawa, K. In vivo anticlastogenic and antimutagenic effects of tannic acid in mice. *Mutat. Res. Lett.* **1990**, *244*, 43–47. [[CrossRef](#)] [[PubMed](#)]
- Youness, R.A.; Kamel, R.; Elkasabgy, N.A.; Shao, P.; Farag, M.A. Recent Advances in Tannic Acid (Gallotannin) Anticancer Activities and Drug Delivery Systems for Efficacy Improvement: A Comprehensive Review. *Molecules* **2021**, *26*, 1486. [[CrossRef](#)]
- Baer-Dubowska, W.; Szaefer, H.; Majchrzak-Celińska, A.; Krajka-Kuźniak, V. Tannic Acid: Specific Form of Tannins in Cancer Chemoprevention and Therapy-Old and New Applications. *Curr. Pharmacol. Rep.* **2020**, *6*, 28–37. [[CrossRef](#)]

27. Sahiner, M.; Kurt, S.B.; Sahiner, N. Biodiverse Properties of Tannic Acid-Based Fibers. *Fibers Polym.* **2021**, *22*, 2986–2994. [[CrossRef](#)]
28. Jyske, T.; Liimatainen, J.; Tienaho, J.; Brännström, H.; Aoki, D.; Kuroda, K.; Reshamwala, D.; Kunnas, S.; Halmemies, E.; Nakayama, E.; et al. Inspired by nature: Fiber networks functionalized with tannic acid and condensed tannin-rich extracts of Norway spruce bark show antimicrobial efficacy. *Front. Bioeng. Biotechnol.* **2023**, *11*, 1171908. [[CrossRef](#)]
29. Kang, Y.; Li, M.; Han, Y.; Sun, H.; Dan, J.; Liang, Y.; Zhang, Q.; Su, Z.; Yue, T.; Wang, J.; et al. Tannic acid-derived selective capture of bacteria from apple juice. *Food Chem.* **2023**, *412*, 135539. [[CrossRef](#)]
30. Haapakoski, M.; Emelianov, A.; Reshamwala, D.; Laajala, M.; Tienaho, J.; Kilpeläinen, P.; Liimatainen, J.; Jyske, T.; Pettersson, M.; Marjomäki, V. Antiviral functionalization of cellulose using tannic acid and tannin-rich extracts. *Front. Microbiol.* **2023**, *14*, 1287167. [[CrossRef](#)]
31. Deng, L.; Qi, Y.; Liu, Z.; Xi, Y.; Xue, W. Effect of tannic acid on blood components and functions. *Colloids Surf. B Biointerfaces* **2019**, *184*, 110505. [[CrossRef](#)]
32. Basu, T.; Panja, S.; Shendge, A.K.; Das, A.; Mandal, N. A natural antioxidant, tannic acid mitigates iron-overload induced hepatotoxicity in Swiss albino mice through ROS regulation. *Environ. Toxicol.* **2018**, *33*, 603–618. [[CrossRef](#)] [[PubMed](#)]
33. Salman, M.; Tabassum, H.; Parvez, S. Tannic Acid Provides Neuroprotective Effects Against Traumatic Brain Injury Through the PGC-1 $\alpha$ /Nrf2/HO-1 Pathway. *Mol. Neurobiol.* **2020**, *57*, 2870–2885. [[CrossRef](#)] [[PubMed](#)]
34. Yeo, J.; Lee, J.; Yoon, S.; Kim, W.J. Tannic acid-based nanogel as an efficient anti-inflammatory agent. *Biomater. Sci.* **2020**, *8*, 1148–1159. [[CrossRef](#)]
35. Chung, K.-T.; Wong, T.Y.; Wei, C.-I.; Huang, Y.-W.; Lin, Y. Tannins and Human Health: A Review. *Crit. Rev. Food Sci. Nutr.* **1998**, *38*, 421–464. [[CrossRef](#)]
36. Baldwin, A.; Booth, B.W. Biomedical applications of tannic acid. *J. Biomater. Appl.* **2022**, *36*, 1503–1523. [[CrossRef](#)]
37. Jing, W.; Xiaolan, C.; Yu, C.; Feng, Q.; Haifeng, Y. Pharmacological effects and mechanisms of tannic acid. *Biomed. Pharmacother.* **2022**, *154*, 113561. [[CrossRef](#)]
38. Sengel, S.B.; Sahiner, M.; Aktas, N.; Sahiner, N. Halloysite-carboxymethyl cellulose cryogel composite from natural sources. *Appl. Clay Sci.* **2017**, *140*, 66–74. [[CrossRef](#)]
39. Saniner, N.; Suner, S.S.; Tosunoglu, M. Preparation of Macroporous Carboxymethyl Cellulose Cryogels and Its Blood Compatibility. *MRS Adv.* **2020**, *5*, 825–833. [[CrossRef](#)]
40. Can, M.; Sahiner, M.; Sahiner, N. Colloidal bioactive nanospheres prepared from natural biomolecules, catechin and L-lysine. *J. Polym. Res.* **2022**, *29*, 88. [[CrossRef](#)]
41. Mosmann, T. Rapid colorimetric assay for cellular growth and survival: Application to proliferation and cytotoxicity assays. *J. Immunol. Methods* **1983**, *65*, 55–63. [[CrossRef](#)]
42. Zhou, X.; Zhou, Q.; Chen, Q.; Ma, Y.; Wang, Z.; Luo, L.; Ding, Q.; Li, H.; Tang, S. Carboxymethyl Chitosan/Tannic Acid Hydrogel with Antibacterial, Hemostasis, and Antioxidant Properties Promoting Skin Wound Repair. *ACS Biomater. Sci. Eng.* **2023**, *9*, 437–448. [[CrossRef](#)] [[PubMed](#)]
43. Kumar, B.; Priyadarshi, R.; Sauraj; Deeba, F.; Kulshreshtha, A.; Gaikwad, K.K.; Kim, J.; Kumar, A.; Negi, Y.S. Nanoporous Sodium Carboxymethyl Cellulose-g-poly (Sodium Acrylate)/FeCl<sub>3</sub> Hydrogel Beads: Synthesis and Characterization. *Gels* **2020**, *6*, 49. [[CrossRef](#)] [[PubMed](#)]
44. Kumar, B.; Sauraj; Negi, Y.S. To investigate the effect of ester-linkage on the properties of polyvinyl alcohol/carboxymethyl cellulose based hydrogel. *Mater. Lett.* **2019**, *252*, 308–312. [[CrossRef](#)]
45. Zhong, X.; Ji, C.; Chan, A.K.L.; Kazarian, S.G.; Ruys, A.; Dehghani, F. Fabrication of chitosan/poly( $\epsilon$ -caprolactone) composite hydrogels for tissue engineering applications. *J. Mater. Sci. Mater. Med.* **2011**, *22*, 279–288. [[CrossRef](#)]
46. Kirillova, A.; Yeazel, T.R.; Asheghali, D.; Petersen, S.R.; Dort, S.; Gall, K.; Becker, M.L. Fabrication of Biomedical Scaffolds Using Biodegradable Polymers. *Chem. Rev.* **2021**, *121*, 11238–11304. [[CrossRef](#)]
47. Torgbo, S.; Sukyai, P. Biodegradation and thermal stability of bacterial cellulose as biomaterial: The relevance in biomedical applications. *Polym. Degrad. Stab.* **2020**, *179*, 109232. [[CrossRef](#)]
48. Song, R.; Murphy, M.; Li, C.; Ting, K.; Soo, C.; Zheng, Z. Current development of biodegradable polymeric materials for biomedical applications. *Drug Des. Dev. Ther.* **2018**, *12*, 3117–3145. [[CrossRef](#)]
49. Fujimori, S. Gastric acid level of humans must decrease in the future. *World J. Gastroenterol.* **2020**, *26*, 6706–6709. [[CrossRef](#)]
50. Gaohua, L.; Miao, X.; Dou, L. Crosstalk of physiological pH and chemical pKa under the umbrella of physiologically based pharmacokinetic modeling of drug absorption, distribution, metabolism, excretion, and toxicity. *Expert Opin. Drug Metab. Toxicol.* **2021**, *17*, 1103–1124. [[CrossRef](#)]
51. Yamamura, R.; Inoue, K.Y.; Nishino, K.; Yamasaki, S. Intestinal and fecal pH in human health. *Front. Microbiomes* **2023**, *2*, 1192316. [[CrossRef](#)]
52. Urbán, P.; Liptrott, N.J.; Bremer, S. Overview of the blood compatibility of nanomedicines: A trend analysis of in vitro and in vivo studies. *WIREs Nanomed. Nanobiotechnology* **2019**, *11*, e1546. [[CrossRef](#)] [[PubMed](#)]
53. Hedayati, M.; Neufeld, M.J.; Reynolds, M.M.; Kipper, M.J. The quest for blood-compatible materials: Recent advances and future technologies. *Mater. Sci. Eng. R Rep.* **2019**, *138*, 118–152. [[CrossRef](#)]
54. Xu, L.-C.; Bauer, J.W.; Siedlecki, C.A. Proteins, platelets, and blood coagulation at biomaterial interfaces. *Colloids Surfaces B Biointerfaces* **2014**, *124*, 49–68. [[CrossRef](#)] [[PubMed](#)]

55. Ohta, S.; Nishiyama, T.; Sakoda, M.; Machioka, K.; Fuke, M.; Ichimura, S.; Inagaki, F.; Shimizu, A.; Hasegawa, K.; Kokudo, N.; et al. Development of carboxymethyl cellulose nonwoven sheet as a novel hemostatic agent. *J. Biosci. Bioeng.* **2015**, *119*, 718–723. [[CrossRef](#)]
56. Lippi, G.; Favalaro, E.J.; Franchini, M. Haemolysis index for the screening of intravascular haemolysis: A novel diagnostic opportunity? *Blood Transfus.* **2018**, *16*, 433–437. [[CrossRef](#)]
57. Fromer, D.L.; Cheng, W.Y.; Gao, C.; Mahendran, M.; Hilt, A.; Duh, M.S.; Joshi, A.V.; Mulgirigama, A.; Mitrani-Gold, F.S. Likelihood of Antimicrobial Resistance in Urinary E. coli Isolates among US Female Patients with Recurrent versus Non-Recurrent uUTI. *Urology* **2024**, *190*, 1–10. [[CrossRef](#)]
58. Qin, L.; Hu, N.; Zhang, Y.; Yang, J.; Zhao, L.; Zhang, X.; Yang, Y.; Zhang, J.; Zou, Y.; Wei, K.; et al. Antibody-antibiotic conjugate targeted therapy for orthopedic implant-associated intracellular S. aureus infections. *J. Adv. Res.* **2023**, *65*, 239–255. [[CrossRef](#)]
59. André, C.; Lebreton, F.; Van Tyne, D.; Cadorette, J.; Boody, R.; Gilmore, M.S.; Bispo, P.J.M. Microbiology of Eye Infections at the Massachusetts Eye and Ear: An 8-Year Retrospective Review Combined With Genomic Epidemiology. *Am. J. Ophthalmol.* **2023**, *255*, 43–56. [[CrossRef](#)]

**Disclaimer/Publisher’s Note:** The statements, opinions and data contained in all publications are solely those of the individual author(s) and contributor(s) and not of MDPI and/or the editor(s). MDPI and/or the editor(s) disclaim responsibility for any injury to people or property resulting from any ideas, methods, instructions or products referred to in the content.